

The use of methylsalicyloxime in manganese chemistry: A $[\text{Mn}_3^{\text{III}}]$ triangle and its oxidation to a $[\text{Mn}_4^{\text{IV}}\text{Ce}_2^{\text{III}}]$ rod

Constantinos J. Milios^a, Peter A. Wood^a, Simon Parsons^a, Dolos Foguet-Albiol^b, Christos Lampropoulos^b, George Christou^b, Spyros P. Perlepes^c, Euan K. Brechin^{a,*}

^a School of Chemistry, The University of Edinburgh, West Mains Road, Edinburgh EH9 3JJ, UK

^b Department of Chemistry, University of Florida, Gainesville, FL 32611-7200, USA

^c Department of Chemistry, University of Patras, 26504 Patras, Greece

Received 27 November 2006; received in revised form 4 June 2007; accepted 8 June 2007

Available online 30 June 2007

Paper presented in the MAGMANet-ECMM, European Conference on Molecular Magnetism.

Abstract

The preparation, crystal structure and reactivity of a trimetallic Mn^{III} carboxylate cluster containing the dianion of methylsalicyloxime (Me-saoH_2), is reported. The reaction between $\text{Mn}(\text{OAc})_2 \cdot 4\text{H}_2\text{O}$ and Me-saoH_2 in pyridine (py) produces the complex $[\text{Mn}_3^{\text{III}}\text{O}(\text{OAc})(\text{Me-sao})_3(\text{py})_4] \cdot 2\text{py}$ (**1** · 2py) in very good yields. The neutral complex consists of a central triangular $\{\text{Mn}_3^{\text{III}}\text{O}\}$ unit assembled together by three $\eta^1:\eta^1:\eta^1:\mu_2$ -oximato(−2) and one bridging AcO^- ligands. Oxidation of **1** · 2 py in MeCN in the presence of $(\text{NH}_4)_2[\text{Ce}^{\text{IV}}(\text{NO}_3)_6]$ leads to the formation of complex $[\text{Mn}_4^{\text{IV}}\text{Ce}_2^{\text{III}}\text{O}_2(\text{Me-sao})_6(\text{NO}_3)_4(\text{OAc})_2(\text{H}_2\text{O})_2] \cdot 6\text{MeCN}$ (**2** · 6MeCN). Its centrosymmetric structure may be described as two $\{\text{Mn}_2^{\text{IV}}\text{Ce}^{\text{III}}\text{O}\}$ triangles linked through two $\eta^2:\eta^2:\eta^1:\mu_4$ oximato(−2) ligands. Each $\{\text{Mn}_2^{\text{IV}}\text{Ce}^{\text{III}}\text{O}\}$ unit is held together via one $\eta^2:\eta^1:\eta^1:\mu_3$ and one $\eta^1:\eta^1:\eta^1:\mu_2$ - Me-sao^{2-} ligand, and one bridging acetate. Dc magnetic susceptibility studies reveal the presence of dominant antiferromagnetic interactions in both complexes.

© 2007 Elsevier B.V. All rights reserved.

Keywords: Crystal structures; Methylsalicyloximate ligand; Magnetochemistry; Manganese(IV)/cerium(III) clusters; Oxo-centred manganese(III) triangles

1. Introduction

The employment of new ligands towards the synthesis of new homometallic and heterometallic species is of great significance for the future of coordination chemistry and its interface with multidisciplinary fields of science such as bioinorganic chemistry, materials science and magnetochemistry [1]. It is not an exaggeration to state that the design of ligands underlines much of modern coordination chemistry. Important tools for the development of new synthetic patterns and strategies are the ligands used, which

may lead to metallic complexes with potential technological applications. For example, in the field of molecular magnetism, new types of ligands have led to the formation of complexes that display single-molecule magnetism, in an attempt to mimic or improve the behaviour of the prototype Mn_{12}OAc complex [2]. This molecule is able to retain its magnetization in the absence of an external magnetic field, once magnetized at very low temperatures, for prolonged periods of time due to the presence of a high-spin ground-state, S , and a large and negative magnetoanisotropy, D , that establishes an energy barrier for the re-orientation of the magnetization equal to $U = S^2|D|$. Of great importance for the development of this particular area of molecular magnetism is the synthesis of new poly-metallic compounds and the study of their magnetic

* Corresponding author. Tel.: +44 131 650 7545.

E-mail address: ebrechin@staffmail.ed.ac.uk (E.K. Brechin).

properties. Since the discovery of the prototype molecule, numerous compounds have been found to display SMM behaviour and this has led to a better understanding of the fundamental principles that govern this remarkable phenomenon [3].

For several years we have focused our interest on the study of homometallic complexes of oximate ligands since they have proven a fruitful source of polynuclear complexes (clusters), displaying a range of magnetic properties from high-spin molecules to SMMs [4,5]. This investigation was initiated as an attempt to discover the “chemistry” of oximes that present “structural similarity” to di-2-pyridyl ketone, (py)₂CO (Scheme 1), since – from our previous experience – (py)₂CO had proven to be an excellent candidate for the formation of polynuclear clusters [M_x] (M = Mn, Fe, Co, Ni, Cu; x = 3–14) [6]. The first oximes employed were di-2-pyridyl ketone oxime, (py)₂CNOH, phenyl 2-pyridyl ketone oxime, (py)C(ph)NOH, and 2-pyridinealdoxime, (py)C(H)NOH; we also employed salicylaldoxime (saoH₂) (Scheme 1). Even though oxime species cannot be considered “new” ligands in coordination chemistry [5,7], they have been used (for example) as models for the biologically important imidazole donor group of the amino acid histidine [8], as corrosion inhibitors [9] and as copper extractants in metallurgical procedures [10]. We

feel that they may play an important, and perhaps even leading role, in the synthesis of the next generation of SMMs.

In this paper, we will restrict our discussion to saoH₂ and its analogues. We believed that this ligand offered the potential for easy functionalisation, allowing us to vary the steric and electronic properties of the resulting complexes systematically. Recently, we reported that upon functionalising the oxime carbon of saoH₂ with an Et-group (to form Et-saoH₂, Scheme 1), we were able to tune the ground-state of a [Mn₆^{III}] SMM [4g] from *S* = 4 to *S* = 12 preparing a molecule with *U*_{eff} = ~53 K, due to the imposed twisting of the bridging moiety [11] and the resultant structural distortion this caused. Herein, we report the synthesis of a [Mn₃^{III}] triangle featuring the newest member of the oximes under study, Me-saoH₂ (Scheme 1), and its Ce^{IV}-assisted oxidation to form a heterometallic [Mn₄^{IV}Ce₂^{III}] complex. The use of Me-saoH₂ in manganese chemistry seems very promising, since it has already provided the first ferromagnetic [Mn₄^{III}] cube displaying SMM behaviour [12].

2. Experimental

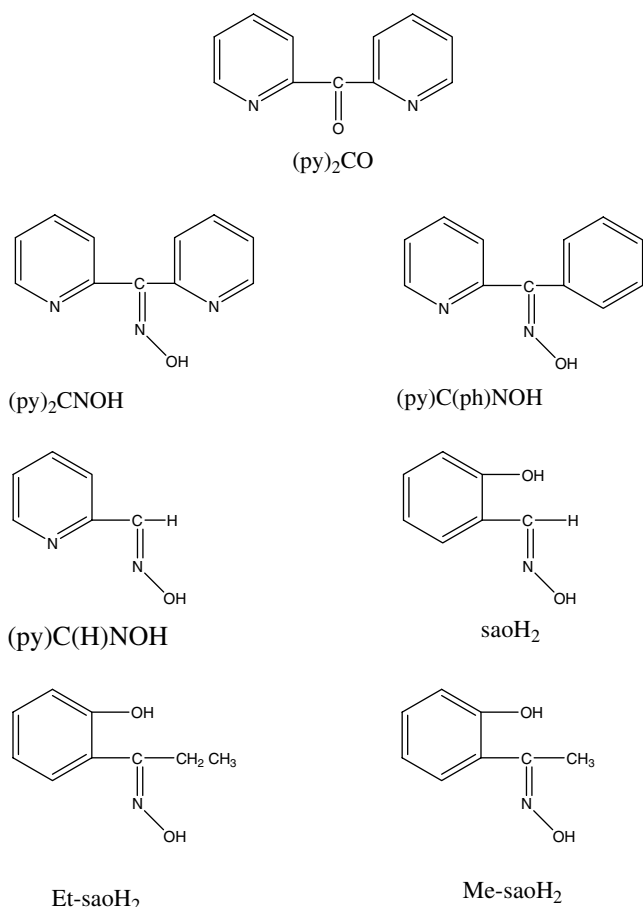
2.1. General and physical measurements

All manipulations were performed under aerobic conditions using materials (reagent grade) and solvents as received. Me-saoH₂ was prepared as described elsewhere [13]. Elemental analyses (C, H, N) were performed by the EaStCHEM microanalysis service. IR spectra (4000–450 cm⁻¹) were recorded as KBr pellets on a Jasco FT/IR-410 spectrometer. Variable-temperature, solid-state direct current (dc) magnetic susceptibility data down to 5 K were collected on a Quantum Design MPMS-XL SQUID magnetometer equipped with a 7 T dc magnet. Diamagnetic corrections were applied to the observed paramagnetic susceptibilities using Pascal’s constants.

2.2. Compound preparation

2.2.1. [Mn₃^{III}O(OAc)(Me-sao)₃(py)₄] · 2py (I · 2py)

A white suspension of Mn(OAc)₂ · 4H₂O (245 mg, 1.0 mmol) in py (20 ml) was treated with solid Me-saoH₂ (151 mg, 1 mmol) in the presence of NEt₃ (0.6 ml). After 1 h of stirring, the resulting dark brown suspension was filtered and the dark brown solution was left to slowly evaporate at room temperature. X-ray quality black crystals formed during 3 days. The crystals were collected by filtration, washed with Et₂O (2 × 4 ml) and dried *in vacuo*. The yield was approximately 45%. The dried sample analyzed as solvent-free. *Anal.* Calc. for C₄₆H₄₄Mn₃N₇O₉: C, 55.03; H, 4.42; N, 9.77. Found: C 55.12; H 4.30; N 9.63%. IR data (KBr pellet, cm⁻¹): 1592 s, 1561 s, 1525 s, 1482 s, 1435 s, 1365 s, 1319 s, 1249 m, 1212 m, 1133 m, 1051s, 1028 s, 972 s, 864 s, 809 w, 749 s, 703 s, 674 s, 641 s, 616 w, 594 w, 570 w, 546 w, 520 w, 474 m, 434 s, 417 w.



Scheme 1. The ligands discussed in the text.

2.2.2. $[\text{Mn}_4^{\text{IV}}\text{Ce}_2^{\text{III}}\text{O}_2(\text{Me-sao})_6(\text{NO}_3)_4(\text{OAc})_2(\text{H}_2\text{O})_2] \cdot 6\text{MeCN} (2 \cdot 6\text{MeCN})$

To a stirred brown suspension of $1 \cdot 2\text{py}$ (581 mg, 0.5 mmol) in MeCN (40 ml), was added solid $(\text{NH}_4)_2[\text{Ce}(\text{NO}_3)_6]$ (274 mg, 0.5 mmol) and the suspension was stirred for 3 h, during which time the $(\text{NH}_4)_2[\text{Ce}(\text{NO}_3)_6]$ dissolved. The resulting dark brown suspension was filtered and left for slow evaporation. After 5 days, single crystals suitable for X-ray diffraction formed. The crystals were collected by filtration, washed with Et_2O (2×3 ml) and dried *in vacuo*. The yield was approximately 35%. The dried sample analyzed as $2 \cdot 2\text{MeCN}$. *Anal.* Calc. for $\text{C}_{56}\text{H}_{58}\text{Ce}_2\text{Mn}_4\text{N}_{12}\text{O}_{32}$: C, 35.19; H, 3.06; N, 8.79. Found: C, 35.31; H, 3.25; N, 8.63%. IR data (KBr pellet, cm^{-1}): 1593 w, 1566 w, 1435 w, 1383 s, 1338 m, 1300 m, 1132 m, 1073 w, 1049 m, 1027 w, 974 s, 856 s, 814 w, 759 s, 672 s, 638 m, 577 m, 556 m, 518 w, 480 s, 405 w.

2.3. X-ray crystallography

Diffraction data were collected at 150 K on a Bruker Smart Apex CCD diffractometer equipped with an Oxford Cryosystems LT device. Complete crystal data and parameters for data collection and processing are reported in Table 1. The structures were solved by direct methods (SHELXS) and refined by full-matrix least-squares against F^2 (CRYSTALS) [14]. The hydrogen atoms were placed geometrically, then refined subject to geometric restraints

Table 1
Crystal data and structure refinement for complexes $1 \cdot 2\text{py}$ and $2 \cdot 6\text{MeCN}$

Compound	$1 \cdot 2\text{py}$	$2 \cdot 6\text{MeCN}$
Formula	$\text{C}_{56}\text{H}_{54}\text{Mn}_3\text{N}_9\text{O}_9$	$\text{C}_{64}\text{H}_{70}\text{Ce}_2\text{Mn}_4\text{N}_{16}\text{O}_{32}$
Formula weight	1161.8	2075.36
Crystal system	monoclinic	triclinic
Space group	$P2_1/n$	$P\bar{1}$
<i>Unit cell dimensions</i>		
a (Å)	10.1142(3)	11.7965(4)
b (Å)	22.8891(6)	13.3428(4)
c (Å)	23.1854(7)	14.9432(5)
α (°)	90	110.865(2)
β (°)	96.048(2)	108.038(2)
γ (°)	90	99.869(2)
V (Å ³)	5337.7(3)	1981.97(11)
Z	4	4
D_{calc} (Mg m ⁻³)	1.446	1.739
Temperature (K)	150	150
$F(000)$	2400	1038
θ Range (°)	1.78–28.87	1.59–27.03
Index ranges	$-12 \leq h \leq 13$, $-29 \leq k \leq 30$, $-31 \leq l \leq 29$	$-15 \leq h \leq 15$, $-17 \leq k \leq 17$, $-19 \leq l \leq 18$
Reflections collected	63 548	34 997
Independent reflections (R_{int})	13 070 (0.045)	8 660 (0.0389)
Parameters refined	694	542
R_1^a (data)	0.0400 (7685)	0.0306 (9888)
wR_2^b [$F > 4\sigma(F)$]	0.0742	0.0981
Goodness-of-fit on F^2	0.8970	1.118

^a $R_1 = \sum(|F_o| - |F_c|) / \sum(|F_o|)$.

^b $wR_2 = \{ \sum[w(F_o^2 - F_c^2)^2] / \sum[w(F_o^2)^2] \}^{1/2}$.

and finally constrained to ride on their host atoms, unless otherwise stated. For compound **2**, H-atoms were placed at calculated positions, except those on O71, which were located in a difference map. The water and methyl groups were treated as rotating rigid groups. The MeCN solvate molecules were restrained to be geometrically similar.

3. Results and discussion

3.1. Syntheses

The 1:1 reaction between $\text{Mn}(\text{OAc})_2 \cdot 4\text{H}_2\text{O}$ and Me-saoH_2 in py, in the presence of NET_3 , yields complex $[\text{Mn}_3\text{O}(\text{OAc})(\text{Me-sao})_3(\text{py})_4]$ (**1**). The neutral complex was crystallographically identified as $1 \cdot 2\text{py}$. All manganese atoms are in the 3+ oxidation state and **1** may be considered as a member of the large family of oxo-centred $[\text{Mn}_3\text{O}]$ triangles [15]. The role of NET_3 is dual: it helps the deprotonation of the oxime ligand, as well as the rapid oxidation (in air) of the Mn^{II} starting material, since it is well-known that higher pH values favour the formation of Mn^{III} ions. The same product can also be isolated in the absence of base, but longer periods of stirring are required in order for Mn^{II} to be oxidized to Mn^{III} , as is evidenced from the colour of the solution which darkens only slowly upon stirring. The nature of the base is not crucial for the identity of the product, since we were able to isolate **1** by using a plethora of bases such as NET_3 , NMe_4OH , NET_4OH , NaOH , etc.

Our next synthetic goal was to try to oxidize some of the Mn^{III} ions in **1** to Mn^{IV} ions – with or without strict retention of structure. $(\text{NH}_4)_2[\text{Ce}^{\text{IV}}(\text{NO}_3)_6]$ was selected as the oxidant. Cerium(IV) is commonly employed as an oxidant in inorganic synthesis [16a–c], and has a long history as an oxidizing agent for a vast variety of organic substrates [16d,16e]. The 1:1 reaction between **1** and $(\text{NH}_4)_2[\text{Ce}^{\text{IV}}(\text{NO}_3)_6]$ in MeCN gives the complex $[\text{Mn}_4^{\text{IV}}\text{Ce}_2^{\text{III}}\text{O}_2(\text{Me-sao})_6(\text{NO}_3)_4(\text{OAc})_2(\text{H}_2\text{O})_2]$ (**2**) which was crystallographically identified as $2 \cdot 6\text{MeCN}$. Complex **2** is heterometallic containing both Mn^{IV} and Ce^{III} atoms. Since the yield of **2** was rather small (~35%) and the filtrate – after its isolation – intensely coloured, it is likely, as with many other reactions in Mn chemistry [17], that the reaction solution contains a mixture of several species in equilibrium, with factors such as relative solubility, lattice energies, crystallization kinetics and so on determining the identity of the isolated product. With the identity of complex **2** established, we tried to prepare **2** *in situ* from the 1:1:1 $\text{Mn}(\text{OAc})_2 \cdot 4\text{H}_2\text{O}/\text{Me-saoH}_2/(\text{NH}_4)_2[\text{Ce}(\text{NO}_3)_6]$ reaction mixture in MeCN. We were able to isolate a microcrystalline material which displayed an identical IR spectrum to **2** and analytical data very close to those corresponding to $2 \cdot \text{MeCN}$, but no single-crystals suitable for X-ray crystallography could be made under the conditions investigated.

The $\text{Mn}^{n+}/\text{RCOO}^-/\text{Me-saoH}$ ternary system seems to be of great synthetic potential, since from the 1:1 reaction

of $\text{Mn}(\text{OAc})_2 \cdot 4\text{H}_2\text{O}$ and Me-saoH_2 in MeCN , we were able to isolate and characterize the cube-like complex $[\text{Mn}_4(\text{Me-sao})_4(\text{Me-saoH})_4]$ (**3**) in which all manganese atoms are in the +3 oxidation state [12]. The same reaction in py gave complex **1**, and in the presence of $(\text{NH}_4)_2[\text{Ce}(\text{NO}_3)_6]$ gave complex **2**, therefore suggesting that the system is very sensitive to subtle synthetic parameters such as solvent, base and oxidizing agents.

3.2. Description of structures

The molecular structure of complex **1** is shown in Fig. 1, and selected interatomic distances and angles are given in Table 2. Complex **1** crystallizes in the monoclinic space group $P2_1/n$. Its structure consists of a near-equilateral Mn_3^{III} triangle ‘capped’ by the central oxo ion, O(1). The core of the complex consists of a $[\text{Mn}_3(\mu_3\text{-O})]^{7+}$ moiety, in which the central oxo bridge lies 0.35 Å above the plane defined by the three manganese ions, in contrast to the vast majority of triangular $[\text{Mn}_3(\mu_3\text{-O})]^{6+/7+}$ species in which the central oxo group and the metal ions are coplanar [15]. Such an arrangement has been reported recently and has been suggested to modify the magnetic behaviour of the complex [18]. Each edge of the triangle is bridged by a diatomic oximate(−1) group of an $\eta^1:\eta^1:\eta^1:\mu_2\text{-Me-sao}^{2-}$ ligand, whose deprotonated hydroxyl group is bound terminally to a Mn^{III} ion. The $\text{Mn}(2)\cdots\text{Mn}(3)$ edge is additionally bridged by the $\eta^1:\eta^1:\mu_2\text{-AcO}^-$ group. Two pyridine ligands complete six-coordination at $\text{Mn}(1)$, while the coordination sphere of $\text{Mn}(2)$ and $\text{Mn}(3)$ is completed by one py molecule. Each metal centre adopts a distorted octahedral geometry.

The oxidation states of the Mn atoms were determined from a combination of charge balance, bond lengths, the presence of $\text{Mn}^{\text{III}}(\text{d}^4)$ Jahn–Teller elongation axes $[\text{N}(14)\text{--}$

$\text{Mn}(1)\text{--N}(15)$, $\text{O}(28)\text{--Mn}(2)\text{--N}(16)$, $\text{O}(38)\text{--Mn}(3)\text{--N}(17)]$ and bond valence sum (BVS) calculations [19]. The BVS calculations are summarized in Table 4. There is no identifiable regular packing pattern and no H-bonds are present. The closest intermolecular $\text{Mn}\cdots\text{Mn}$ distance is ~ 9 Å. Complex **1** joins a rather large family of triangular Mn^{III} complexes containing the $[\text{Mn}_3(\mu_3\text{-O})]^{7+}$ core [15b,15c,18].

The molecular structure of complex **2** is shown in Fig. 2, and selected interatomic distances and angles are given in Table 3. Complex **2** crystallizes in the triclinic space group $P\bar{1}$, with the molecule lying on an inversion centre. The molecule has a novel $[\text{Mn}_4^{\text{IV}}\text{Ce}_2^{\text{III}}(\mu_3\text{-O})_2(\mu_2\text{-OAc})_2(\mu_3\text{-NOR})_2(\mu_2\text{-NOR})_4(\mu_2\text{-OR})_4]^{6+}$ core, whose topology consists of six metal ions arranged as two $\{\text{Mn}_2^{\text{IV}}\text{Ce}^{\text{III}}(\mu_3\text{-O})_2\}$ triangular subunits bridged by two oximate oxygen atoms $[\text{O}(101)$, $\text{O}(101')]$ and two deprotonated hydroxyl oxygen atoms $[\text{O}(11)$, $\text{O}(11')]$ that belong to two $\eta^2:\eta^2:\eta^1:\mu_4\text{-Me-sao}^{2-}$ ligands. Along with the triply bridging oxo ion $[\text{O}(1)$, $\text{O}(1')]$, each heterometallic triangular subunit is held together via one $\eta^2:\eta^1:\eta^1:\mu_3\text{-Me-sao}^{2-}$ ligand, one $\eta^1:\eta^1:\eta^1:\mu_2\text{-Me-sao}^{2-}$ ligand that bridges the two Mn^{IV} atoms, and one $\eta^1:\eta^1:\mu_2\text{-AcO}^-$ ion that bridges $\text{Ce}(1)$ $[\text{Ce}(1')]$ and $\text{Mn}(2)$ $[\text{Mn}(2')]$. Two chelating nitrates and one terminal water molecule complete deca-coordination at each Ce^{III} ion. The Mn^{IV} ions are hexa-coordinate adopting slightly distorted octahedral geometries, while the Ce^{III} ion has a bicapped square antiprismatic geometry. The length of the near-planar heterometallic ‘rod’ is ~ 6.7 Å while the closest intermolecular $\text{M}\cdots\text{M}$ distance is ~ 7.2 Å. The oxidation states of the Mn and Ce atoms were assigned by a combination of charge balance, bond lengths and BVS calculations which are shown in Table 4 [19]. The molecules pack in such a way as to form 1D ‘zig-zag’ like chains through an extensive H-bonding network (Fig. 3). Each hexametallc molecule forms six inter-molecular H-bonds; four between terminal H_2O molecules and nitrate ligands and MeCN solvate molecules; and two between the chelating nitrate ligands and terminal H_2O molecules.

It is somewhat surprising to witness the variety of coordination modes adopted by the doubly-deprotonated Me-sao^{2-} ligand in just one molecule: three distinct coordination modes that bridge up to four metal ions, all of which are in high oxidation states – proving the great versatility (and hence potential) of this and similar ligands in coordination chemistry. These modes are illustrated in Scheme 2. From these three modes only one, namely the $\eta^1:\eta^1:\eta^1:\mu_2$ (C) is present in **1**.

Compound **2** is an extremely rare example of a heterometallic Mn/Ce complex. The previously structurally characterized examples are: (i) $[\text{Mn}_8^{\text{III}}\text{Ce}^{\text{IV}}\text{O}_8(\text{O}_2\text{CMe})_{12}(\text{H}_2\text{O})_4]$ whose structure [20a] consists of a non-planar, saddle-like $[\text{Mn}_8\text{O}_8]^{8+}$ loop attached to the central Ce^{IV} via O^{2-} ions; (ii) $[\text{Mn}_2^{\text{IV}}\text{Ce}^{\text{IV}}\text{O}_3(\text{O}_2\text{CMe})(\text{NO}_3)_4(\text{H}_2\text{O})_2(\text{bpy})_2](\text{NO}_3)$ [20b] which comprises a $[\text{Mn}_2^{\text{IV}}(\mu_2\text{-O})_2(\mu_2\text{-O}_2\text{CMe})]^{3+}$ rhomb linked to a Ce^{IV} atom through a linear O^{2-} bridge (bpy = bipyridine); (iii) $[\text{Mn}_2^{\text{IV}}\text{--}$

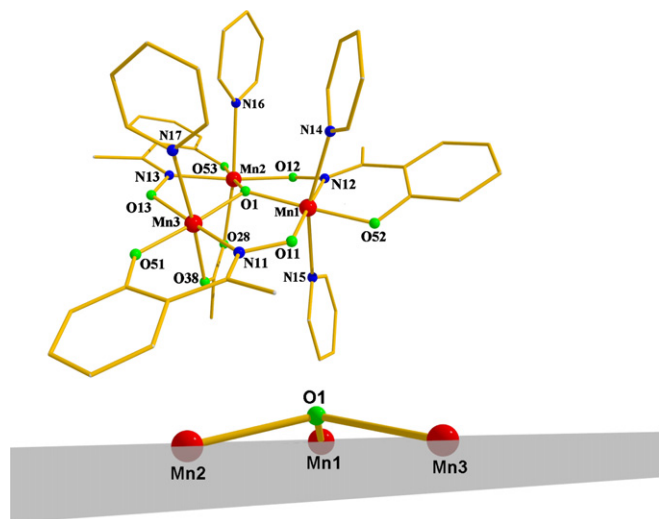


Fig. 1. The molecular structure of complex **1** (top) and the out-of-plane arrangement of the central oxo-group (bottom). The grey plane defines the plane through $\text{Mn}1$, $\text{Mn}2$ and $\text{Mn}3$ (colour code: Mn red, O green, N blue, C yellow).

Table 2
Selected interatomic distances (Å) and angles (°) for complex **1** · 2py

Mn(1)···Mn(2)	3.2390(3)	Mn(2)–N(13)	2.0195(12)
Mn(1)···Mn(3)	3.2387(3)	Mn(2)–O(53)	1.8699(10)
Mn(1)–O(1)	1.8799(10)	Mn(2)–N(16)	2.3908(13)
Mn(1)–O(11)	1.9096(10)	Mn(2)–O(28)	2.1616(11)
Mn(1)–N(12)	2.0112(12)	Mn(3)–O(1)	1.9005(10)
Mn(1)–O(52)	1.8842(10)	Mn(3)–N(11)	2.0148(12)
Mn(1)–N(14)	2.3872(13)	Mn(3)–O(51)	1.8622(10)
Mn(1)–N(15)	2.4213(13)	Mn(3)–O(13)	1.9234(10)
Mn(2)···Mn(3)	3.1785(3)	Mn(3)–N(17)	2.4286(13)
Mn(2)–O(1)	1.8988(10)	Mn(3)–O(38)	2.1519(11)
Mn(2)–O(12)	1.9459(10)		
Mn(2)···Mn(1)···Mn(3)	58.770(7)	O(53)–Mn(2)–N(16)	85.62(5)
O(1)–Mn(1)–O(11)	92.11(4)	N(16)–Mn(2)–O(28)	172.79(4)
O(1)–Mn(1)–N(12)	89.88(5)	O(53)–Mn(2)–O(28)	90.03(4)
O(11)–Mn(1)–N(12)	177.99(5)	Mn(2)···Mn(3)···Mn(1)	60.619(7)
O(1)–Mn(1)–O(52)	178.36(4)	O(1)–Mn(3)–N(11)	90.98(5)
O(11)–Mn(1)–O(52)	89.05(4)	O(1)–Mn(3)–O(51)	176.19(5)
N(12)–Mn(1)–O(52)	88.95(5)	N(11)–Mn(3)–O(51)	90.31(5)
O(1)–Mn(1)–N(14)	95.45(4)	O(1)–Mn(3)–O(13)	92.13(4)
O(11)–Mn(1)–N(14)	91.96(5)	O(1)–Mn(3)–O(38)	91.63(4)
N(12)–Mn(1)–N(14)	87.61(5)	N(11)–Mn(3)–O(38)	93.70(5)
O(1)–Mn(1)–N(15)	100.65(4)	O(51)–Mn(3)–O(38)	91.86(4)
O(11)–Mn(1)–N(15)	94.04(5)	O(13)–Mn(3)–N(17)	85.20(4)
N(12)–Mn(1)–N(15)	85.82(5)	O(13)–Mn(3)–O(38)	93.24(4)
O(52)–Mn(1)–N(14)	83.36(5)	N(17)–Mn(3)–O(38)	176.12(4)
O(52)–Mn(1)–N(15)	80.40(5)	N(11)–Mn(3)–O(13)	172.31(5)
N(14)–Mn(1)–N(15)	162.58(4)	O(1)–Mn(3)–N(17)	91.98(4)
Mn(1)···Mn(2)···Mn(3)	60.610(7)	N(11)–Mn(3)–N(17)	87.67(5)
O(1)–Mn(2)–O(12)	91.68(4)	O(51)–Mn(3)–O(13)	86.15(4)
O(1)–Mn(2)–N(13)	90.84(5)	O(51)–Mn(3)–N(17)	84.49(5)
O(12)–Mn(2)–N(13)	174.34(5)	Mn(3)–O(1)–Mn(2)	113.57(5)
O(1)–Mn(2)–O(53)	176.82(5)	Mn(3)–O(1)–Mn(1)	117.89(5)
O(12)–Mn(2)–O(53)	87.83(4)	Mn(2)–O(1)–Mn(1)	118.00(5)
N(13)–Mn(2)–O(53)	89.37(5)	Mn(1)–O(11)–N(11)	120.69(8)
O(1)–Mn(2)–N(16)	91.23(4)	O(11)–N(11)–Mn(3)	115.52(8)
O(12)–Mn(2)–N(16)	88.29(4)	O(11)–N(11)–C(21)	115.09(12)
N(13)–Mn(2)–N(16)	86.59(5)	Mn(3)–N(11)–C(21)	128.92(10)
O(1)–Mn(2)–O(28)	93.15(4)	N(11)–C(21)–C(31)	120.64(13)
O(12)–Mn(2)–O(28)	97.31(4)	N(11)–C(21)–C(41)	120.76(13)
N(13)–Mn(2)–O(28)	87.62(5)		

$\text{Ce}_3^{\text{IV}}\text{O}_6(\text{O}_2\text{CMe})_6(\text{NO}_3)_2(\text{mhpH})_4$ whose structure [20b] consists of a Ce_3^{IV} isosceles triangle, each edge of which is bridged by two $\mu_3\text{-O}^{2-}$ ions that also bridge to the two Mn^{IV} atoms, each one lying above and below the Ce_3^{IV} triangle forming an M_5 trigonal bipyramid (mhpH 6-methyl-2-hydroxypyridine), and (iv) $[\text{Mn}_6^{\text{IV}}\text{Ce}^{\text{IV}}\text{O}_9(\text{O}_2\text{CMe})_9(\text{MeOH})(\text{H}_2\text{O})](\text{ClO}_4)$ which is a wheel of transition-metal ions housing a central lanthanide ion [20b]. As apparent from the above examples, complex **2** is the first *structurally* characterized complex containing Mn^{IV} and Ce^{III} . It should be mentioned at this point that Ramalakshmi and Rajasekharan [21] have reported the single-crystal X-ray structure of $[\text{Mn}_2^{\text{III,IV}}\text{O}_2(\text{bpy})_4][\text{Ce}^{\text{III}}(\text{NO}_3)_6]$; however, this compound is not a true heterometallic complex but a salt containing separate $[\text{Mn}_2\text{O}_2(\text{bpy})_4]^{3+}$ cations and $[\text{Ce}^{\text{III}}(\text{NO}_3)_6]^{3-}$ anions.

Complexes **1** and **2** join a very small family of structurally characterized metal complexes with anions of Me-saoH_2 as ligands. This family currently comprises the complexes

$[\text{Co}^{\text{III}}(\text{Me-saoH})(\text{NO})]$ [22a], $[\text{Cu}^{\text{II}}(\text{Me-saoH})_2]$ [22b,22c], $[\text{Rh}^{\text{III}}(\text{Me-sao})(\text{Me-saoH})(\text{PPh}_3)_2]$ [22d], $[\text{Ni}(\text{Me-saoH})_2]$ [22e], $[\text{Co}^{\text{II}}(\text{Me-saoH})_2]$ [22f] and $[\text{Mn}_4^{\text{III}}(\text{Me-sao})_4(\text{Me-saoH})_4]$ [12]. In the above-mentioned cobalt, nickel(II), copper(II) and rhodium(III) complexes, the Me-saoH^- and Me-sao^{2-} ions behave as $\text{O}_{\text{phenolate}}$, O_{oxime} or $\text{O}_{\text{oximate}}$ -chelating ligands (in fact the Rh^{III} complex contains the H bonded tri-anion $\text{Me-sao}\cdots\text{H}\cdots\text{Me-sao}^{3-}$ as a $(\text{O}_{\text{phenolate}})_2\text{N}_2$ -chelating ligand). The manganese ‘cube’ [12] contains four $\text{O}_{\text{phenolate}}$, N_{oxime} -chelating Me-saoH^- ligands and four $\eta^1:\eta^2:\eta^1:\mu_3\text{-Me-sao}^{2-}$ ligands. However, unlike the $\eta^2:\eta^1:\eta^1:\mu_3$ mode adopted by two of the Me-sao^{2-} ligands in **2** (**B** in Scheme 2), the bridging donor atom of Me-sao^{2-} in $[\text{Mn}_4^{\text{III}}(\text{Me-sao})_4(\text{Me-saoH})_4]$ is the oximate oxygen [12].

3.3. Magnetic properties

Direct current (dc) magnetic susceptibility studies were performed on a microcrystalline sample of **1** in the

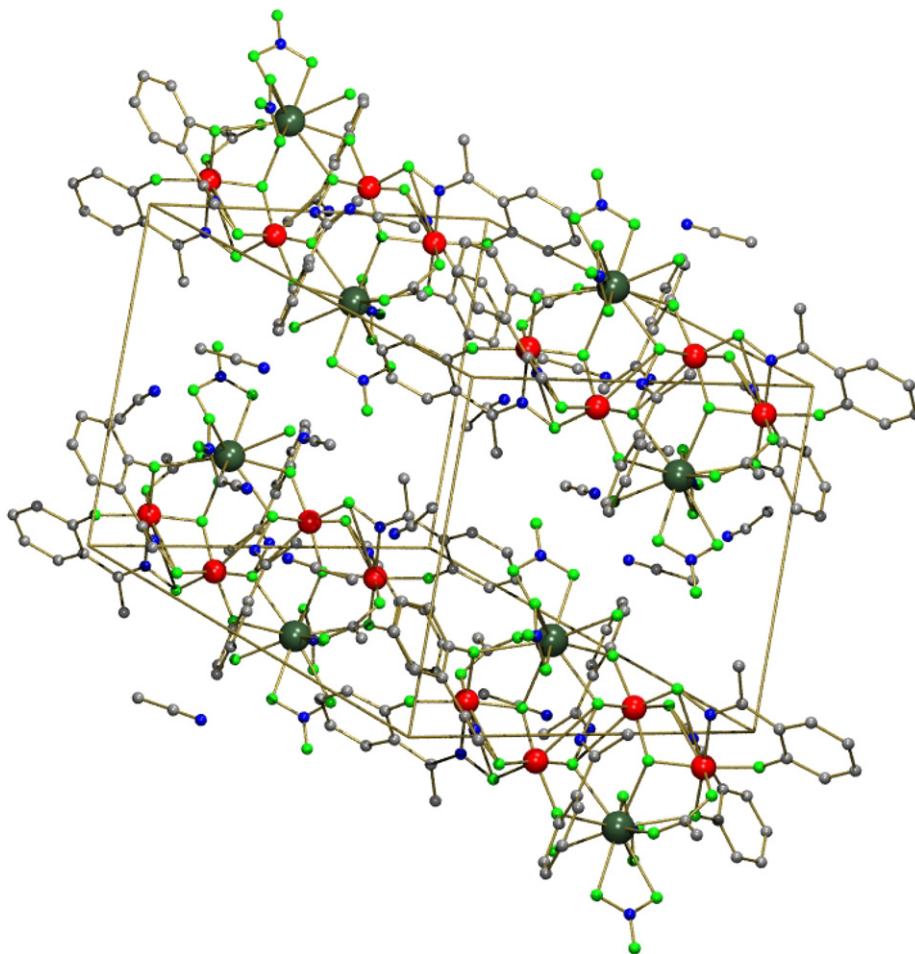
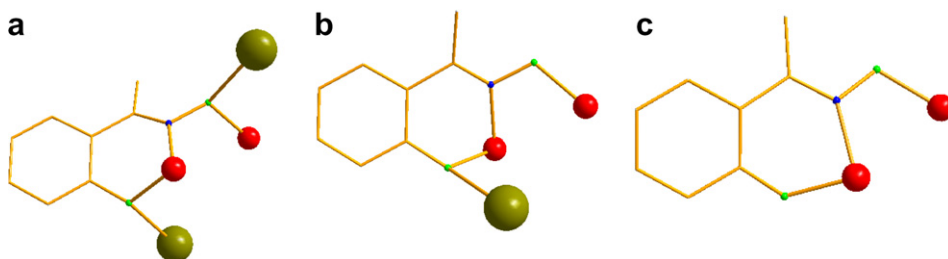


Fig. 3. The crystal packing of complex **2** showing the formation of '1D chains'. The colour scheme is the same as in Fig. 2.



Scheme 2. The coordination modes of the oximato(-2) ligand in **1** and **2**.

and 1.8–10 K and these are plotted as reduced magnetization ($M/N\mu_B$) versus H/T in Fig. 5. The data were fit by a matrix diagonalization method to a model that assumes only the ground state is populated, includes axial zero-field splitting ($D\hat{S}_z^2$) and the Zeeman interaction, and carries out a full powder average. The corresponding Hamiltonian is given in Eq. (2), where D is the axial anisotropy, μ_B is the Bohr magneton, μ_0 is the vacuum permeability, \hat{S}_z is the easy-axis spin operator and H is the applied field:

$$\hat{H} = D\hat{S}_z^2 + g\mu_B\mu_0\hat{S} \cdot H \quad (2)$$

The best fit gave $S = 2$, $g = 1.94$ and $D = -2.43 \text{ cm}^{-1}$. Numerous fits employing only the low field data gave sim-

ilar numbers, while fixing the g -value to 2.0 (spin-only) providing considerably poorer results. Given the weak exchange between the metal centres, the expected presence of a number of low-lying excited states and the likelihood of significant zero-field splitting of the S states, an accurate determination of S and (particularly) $|D|$ via magnetization measurements is difficult and thus inherently inaccurate. Our model assumes population only of the ground state – a scenario which is unlikely to be true, even at the low temperatures employed. The use of only low field data in magnetization versus field fits normally helps to overcome this problem and provide more reliable results. However, in this case all fits produced parameters of similar magnitude

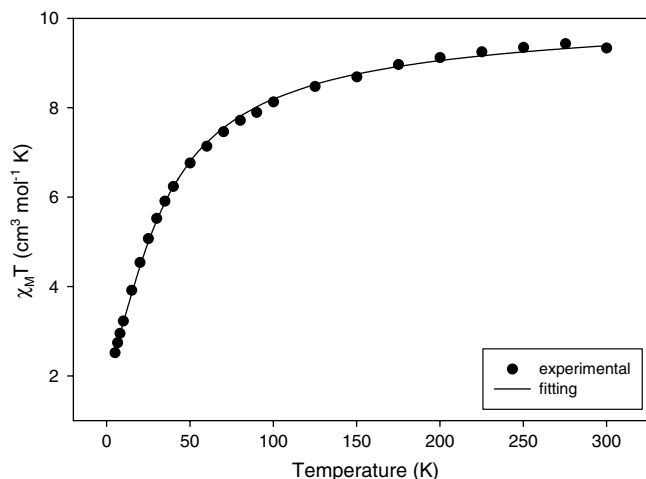


Fig. 4. Plot of $\chi_M T$ vs. T for complex **1**. The solid line represents a fit of the data in the temperature range 300–5 K (see text for details).

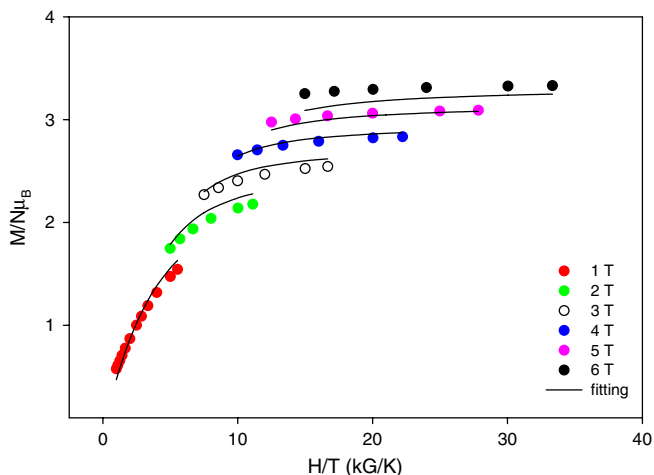


Fig. 5. Plot of reduced magnetization ($M/N\mu_B$) vs. H/T for **1** in fields 1–6 T and temperatures 1.8–10 K.

and goodness of fit. While the magnitude of S is in agreement with the fit of the dc susceptibility data above (and as expected for a $[\text{Mn}_3^{\text{III}}]$ triangle), the validity of the magnitude and sign of $|D|$ is debatable (at best), and a more accurate determination needs to be made from multi-frequency EPR studies. These are currently in progress.

Solid state dc magnetic susceptibility measurements were collected for complex **2** in the temperature range 1.8–300 K in an applied field of 1 kG (see Fig. 6). The room temperature $\chi_M T$ value of approximately $7.4 \text{ cm}^3 \text{ K mol}^{-1}$ (Mn^{4+} , $S = 3/2$; Ce^{3+} , $^2F_{5/2}$, $S = 1/2$, $L = 3$, $J = 5/2$) decreases rather steeply with decreasing temperature to a value of approximately $5.5 \text{ cm}^3 \text{ K mol}^{-1}$ at 150 K, and then ca. $2 \text{ cm}^3 \text{ K mol}^{-1}$ at 10 K before decreasing somewhat more gently to a minimum value of $\sim 1.6 \text{ cm}^3 \text{ K mol}^{-1}$ at 1.8 K. This is indicative of the presence of dominant (and reasonably strong) antiferromagnetic interactions between the four Mn^{4+} ions, with the residual

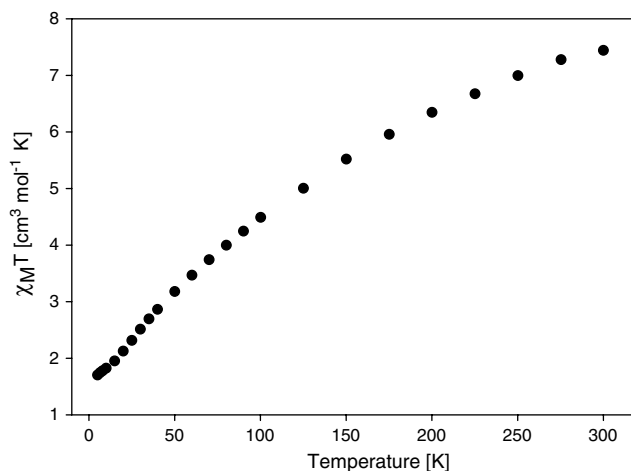


Fig. 6. Plot of $\chi_M T$ vs. T for complex **2** in the temperature range 300–2 K (see text for details).

magnetization at low temperature likely due to the presence of two essentially non-interacting Ce^{3+} ions ($\chi_M T$ value per Ce^{3+} ion, $0.8 \text{ cm}^3 \text{ K mol}^{-1}$).

4. Conclusion

The present work extends the body of results that emphasizes the ability of the dianionic derivatives of salicylaldehyde to form interesting structural types in 3d-transition metal chemistry. The use of Me-saoH₂ in reactions with Mn(II) acetate sources has provided access to three new complexes: (i) the recently reported $[\text{Mn}_4^{\text{III}}]$ distorted cube [12] containing both Me-saoH[−] and Me-sao^{2−} ligands, possessing an $S = 8$ ground state and exhibiting SMM behaviour; (ii) complex **1** reported here which is a rare example of an oxo-centred trimetallic cluster in which the Mn_3^{III} centres are bridged mainly by ligands other than carboxylates, and (iii) complex **2**, also reported in this work, the synthesis of which may “open” a synthetic route to a new class of mixed $\text{Mn}^{\text{IV}}/\text{Ce}^{\text{III}}/\text{O}^{2−}$ molecular clusters. This new procedure has great potential as a route to related species by replacing the Mn and/or Ce for other metal ions. In these three Mn clusters, the ligand Me-sao^{2−} exhibits four different coordination modes (μ_2 , μ_3 , μ_4). This shows that Me-sao^{2−} is a very flexible and versatile ligand for a variety of objectives, including formation of polynuclear complexes (clusters) with other 3d-metal ions, mixed-metal chemistry and magnetochemistry. Thus the future promises many more new and exciting complexes with a host of paramagnetic metal ions including 3d transition metals, combinations of 3d with 4d, 5d and 4f metals, and homometallic 4f-metal clusters.

Acknowledgements

S.P.P. thanks the European Social Fund (ESF), Operational Program for Educational and Vocational Training (EPEAEK II), and particularly the Program PYTHAGO-

RAS I (Grant b. 365.037) for funding the above work. E.K.B. thanks the EPSRC and Leverhulme Trust (UK). G.C. thanks the NSF.

Appendix A. Supplementary material

CCDC 628200 and 628201 contain the supplementary crystallographic data (excluding structure factors) for **1**·2py and **2**·6MeCN. These data can be obtained free of charge via <http://www.ccdc.cam.ac.uk/conts/retrieving.html>, or from the Cambridge Crystallographic Data Centre, 12 Union Road, Cambridge CB2 1EZ, UK; fax: (+44) 1223-336-033; or e-mail: deposit@ccdc.cam.ac.uk. Supplementary data associated with this article can be found, in the online version, at [doi:10.1016/j.ica.2007.06.031](https://doi.org/10.1016/j.ica.2007.06.031).

References

- [1] See the various articles of Section 1 in J.A. McCleverty, T.J. Meyer (Eds.), *Comprehensive Coordination Chemistry II*, vol. 1, Elsevier, Amsterdam, 2004.
- [2] For excellent reviews, see: (a) D. Gatteschi, R. Sessoli, *Angew. Chem., Int. Ed.* 42 (2003) 268; (b) G. Christou, D. Gatteschi, D.N. Hendrickson, R. Sessoli, *MRS Bull.* 25 (2000) 66; (c) R. Bircher, G. Chaboussant, C. Dobe, H.U. Güdel, S.T. Oshsenbein, A. Sieber, O. Waldmann, *Adv. Funct. Mater.* 16 (2006) 209.
- [3] For a comprehensive review, see: G. Aromí, E.K. Brechin, *Struct. Bond.* 122 (2006) 1.
- [4] (a) C.J. Milios, P. Kyritsis, C.P. Raptopoulou, A. Terzis, R. Vicente, S.P. Perlepes, *Dalton Trans.* (2005) 501; (b) C.J. Milios, T.C. Stamatatos, P. Kyritsis, A. Terzis, C.P. Raptopoulou, R. Vicente, A. Escuer, S.P. Perlepes, *Eur. J. Inorg. Chem.* (2004) 2885; (c) C.J. Milios, C.P. Raptopoulou, A. Terzis, R. Vicente, A. Escuer, S.P. Perlepes, *Inorg. Chem. Commun.* 6 (2003) 1056; (d) C.J. Milios, E. Kefalloniti, C.P. Raptopoulou, A. Terzis, A. Escuer, R. Vicente, S.P. Perlepes, *Polyhedron* 23 (2004) 83; (e) C.J. Milios, S. Piligkos, A.R. Bell, R.H. Laye, S.J. Teat, R. Vicente, E. McInnes, A. Escuer, S.P. Perlepes, R.E.P. Winpenny, *Inorg. Chem. Commun.* 9 (2006) 638; (f) C. Papantriantafyllopoulou, C.P. Raptopoulou, A. Escuer, C.J. Milios, *Inorg. Chim. Acta* 360 (2007) 61; (g) C.J. Milios, C.P. Raptopoulou, A. Terzis, F. Lloret, R. Vicente, S.P. Perlepes, A. Escuer, *Angew. Chem., Int. Ed.* 43 (2004) 210; (h) I.A. Gass, C.J. Milios, A.G. Whittaker, F.P.A. Fabiani, S. Parsons, M. Murrie, S.P. Perlepes, E.K. Brechin, *Inorg. Chem.* 45 (2006) 5281; (i) C.J. Milios, A. Vinslava, A.G. Whittaker, S. Parsons, W. Wernsdorfer, G. Christou, S.P. Perlepes, E.K. Brechin, *Inorg. Chem.* 45 (2006) 5272.
- [5] For a review, see: C.J. Milios, Th.C. Stamatatos, S.P. Perlepes, *Polyhedron* 25 (2006) 134 (*Polyhedron Report*).
- [6] (a) C.J. Milios, E. Kefalloniti, C.P. Raptopoulou, A. Terzis, R. Vicente, N. Lalioti, A. Escuer, S.P. Perlepes, *Chem. Commun.* (2003) 819; For a review, see: (b) G.S. Papaefstathiou, S.P. Perlepes, *Comments Inorg. Chem.* 23 (2002) 249.
- [7] For excellent recent reviews, see: (a) A.G. Smith, P.A. Tasker, D.J. White, *Coord. Chem. Rev.* 241 (2003) 61; (b) P. Chaudhuri, *Coord. Chem. Rev.* 243 (2003) 143; (c) A.J.L. Pombeiro, V.Yu. Kukushkin, in: J.A. McCleverty, T.C. Meyer (Eds.), *Comprehensive Coordination Chemistry II*, vol. 1, Elsevier, Amsterdam, 2004, p. 631.
- [8] D.T. Rosa, J.A. Krause Bauer, M.J. Baldwin, *Inorg. Chem.* 40 (2001) 1606.
- [9] J.M. Thorpe, R.L. Beddoes, D. Collison, C.D. Garner, M. Helliwell, J.M. Holmes, P.A. Tasker, *Angew. Chem., Int. Ed.* 38 (1999) 119.
- [10] (a) J. Szymanowski, *Hydroxyoximes and Copper Hydrometallurgy*, CRC Press, Boca Raton, FL, 2000; (b) P.A. Tasker, P.G. Plieger, L.C. West, in: J.A. McCleverty, T.J. Meyer (Eds.), *Comprehensive Coordination Chemistry II*, vol. 9, Elsevier, Amsterdam, 2004, p. 759.
- [11] C.J. Milios, A. Vinslava, P.A. Wood, S. Parsons, W. Wernsdorfer, G. Christou, S.P. Perlepes, E.K. Brechin, *J. Am. Chem. Soc.* 129 (2007) 8.
- [12] C.J. Milios, A. Prescimone, A. Mishra, S. Parsons, W. Wernsdorfer, G. Christou, S.P. Perlepes, E.K. Brechin, *Chem. Commun.* [doi:10.1039/b611174b](https://doi.org/10.1039/b611174b).
- [13] W.R. Dunsten, T.A. Henry, *J. Chem. Soc.* 75 (1899) 66.
- [14] P.W. Betteridge, J.R. Caruthers, R.I. Cooper, K. Prout, D.J. Watkin, *J. Appl. Crystallogr.* 36 (2003) 1487.
- [15] (a) J.B. Vincent, H.R. Chang, K. Foltling, J.C. Huffman, G. Christou, D.N. Hendrickson, *J. Am. Chem. Soc.* 109 (1987) 5703, and references cited therein; For an excellent review, see: (b) D.P. Kessissoglou, *Coord. Chem. Rev.* 185–186 (1999) 837; For a comprehensive review, see: (c) R.D. Cannon, R.P. White, *Prog. Inorg. Chem.* 36 (1988) 195; (d) L.F. Jones, G. Rajaraman, J. Brockman, M. Murugesu, E.C. Sañudo, J. Raftery, S.J. Teat, W. Wernsdorfer, G. Christou, E.K. Brechin, D. Collison, *Chem. Eur. J.* 10 (2004) 5180.
- [16] (a) K.R. Reddy, M.V. Rajasekharan, S. Padhye, F. Dahan, J.-P. Tuchagues, *Inorg. Chem.* 33 (1994) 428; (b) K.R. Reddy, M.V. Rajasekharan, N. Arulsamy, D.J. Hodgson, *Inorg. Chem.* 35 (1996) 2283; (c) K. Dimitrou, A.D. Brown, T.E. Concolino, A.L. Rheingold, G. Christou, *Chem. Commun.* (2001) 1284; (d) B.B. Snider, *Chem. Rev.* 96 (1996) 339; (e) V. Nair, J. Mathew, J. Prabhakaran, *Chem. Soc. Rev.* 26 (1997) 127.
- [17] N.C. Harden, M.A. Bolcar, W. Wernsdorfer, K.A. Abboud, W.E. Streib, G. Christou, *Inorg. Chem.* 42 (2003) 7067.
- [18] Th.C. Stamatatos, D. Foguet-Albiol, C.C. Stoumpos, C.P. Raptopoulou, A. Terzis, W. Wernsdorfer, S.P. Perlepes, G. Christou, *J. Am. Chem. Soc.* 127 (2005) 15380.
- [19] (a) H.H. Thorpe, *Inorg. Chem.* 31 (1992) 1585; (b) W. Liu, H.H. Thorpe, *Inorg. Chem.* 32 (1993) 4102; (c) P.L. Roulhac, G.J. Palenik, *Inorg. Chem.* 42 (2003) 118.
- [20] (a) A.J. Tasiopoulos, W. Wernsdorfer, B. Moulton, M.J. Zaworotko, G. Christou, *J. Am. Chem. Soc.* 125 (2003) 15274; (b) A.J. Tasiopoulos, T.A. O'Brien, K.A. Abboud, G. Christou, *Angew. Chem., Int. Ed.* 43 (2004) 345.
- [21] D. Ramalakshmi, M.V. Rajasekharan, *Acta Crystallogr., Sect. B* 55 (1999) 186.
- [22] (a) L.F. Larkworthy, D.C. Povey, *J. Crystallogr. Spectrosc. Res.* 13 (1983) 413; (b) Z. Kangjing, Z. Chengming, C. Xing, Y. Chengye, *Kexue Tongbao (Chin.) (Chin. Sci. Bull.)* 30 (1985) 266; (c) Z. Kangjing, Z. Chengming, C. Xing, Y. Chengye, *Kexue Tongbao (Chin.) (Chin. Sci. Bull.)* 30 (1985) 1484; (d) R. Acharyya, F. Basuli, G. Rosair, S. Bhattacharya, *New J. Chem.* 28 (2004) 115; (e) A.G. Hatzidimitriou, M. Uddin, M. Lalia-Kantouri, *Z. Anorg. Allg. Chem.* 623 (1997) 627; (f) H.-L. Xiao, F.-F. Jian, *Acta Crystallogr., Sect. E* 62 (2006) m1512.